Available online at www.sciencedirect.com

ScienceDirect

journal homepage: www.intl.elsevierhealth.com/journals/dema

Calcium phosphate coatings elaborated by the soaking process on titanium dental implants: Surface preparation, processing and physical–chemical characterization

Camille Pierre[a,*], *Ghislaine Bertrand*[a], *Christian Rey*[a], *Olivier Benhamou*[b], *Christèle Combes*[a]

[a] *CIRIMAT, Université de Toulouse, CNRS, INP — ENSIACET, 4 allée Emile Monso — BP44362, 31030 Toulouse Cedex 4, France*

[b] *Arts Loi Dental Clinic, Rue de la Loi 28, 1040 Bruxelles, Belgium*

ARTICLE INFO

Article history:
Received 23 February 2018
Received in revised form
4 September 2018
Accepted 11 October 2018

Keywords:
Dental implants
Titanium surface
Calcium phosphates
Coating
Soaking process
Characterization

ABSTRACT

Objective. Dental implant manufacturers are looking for new surfaces to improve osseointegration. It is accepted that calcium phosphate coatings favor bone healing. Among all the techniques, the soaking process seems attractive because of its ability in producing a bioactive coating at low temperature. The objective of this study is to improve the titanium implant surface roughness and chemistry by optimizing the surface preparation and the soaking process parameters to produce a bioactive and adherent calcium phosphate coating.

Methods. Titanium samples were sandblasted and acid etched. Coatings were realized by an alternate soaking process including a centrifugation step to create a phosphate solution thin film on the implant that reacts with the calcium of the second bath. We performed a characterization of the sample surface with complementary physical and physico-chemical techniques to assess the effect of surface preparation and coating process operating parameters on coating formation and characteristics.

Results. Surface preparation led to a roughness around 1.6 μm, micro-porosities, high surface wettability and removed the embedded sandblasting particles. We showed that the centrifugation step is critical and determines the coating formation, coverage and thickness. A thin coating (~2 μm) composed of apatite analogous to bone mineral was deposited. The coating adhesion was demonstrated by screwing/unscrewing test in an artificial jawbone.

Significance. The titanium dental implant pre-treatment and coating developed in this study is expected to favor early implant osseointegration through coating dissolution in vivo and could be associated with biological active agents to confer additional functionality to the coating.

* *Corresponding author.*
E-mail address: camille.pierre@ensiacet.fr (C. Pierre).
https://doi.org/10.1016/j.dental.2018.10.005

1. Introduction

Dental implants provide a good solution for the replacement of tooth roots. Indeed, dental implants restore the functional symmetry of dentition and thus help to maintain the jawbone density and shape, eating and talking ability and smiling aesthetic. All these functions support the psychological, social and physical well-being of the patient. Nevertheless, a long time for bone healing (3–6 months) is required between the implantation and the positioning of the crown (artificial tooth) on the dental implant, which fully reestablish the function of the tooth. Therefore, studies have been carried out to improve implant osseointegration. This characteristic is directly related to the properties of the implant surface that is in close contact with the living bone [1].

Commercially pure titanium (cpTi) and its alloys are widely used for dental implant manufacturing. It has been shown that the roughness and wettability of the titanium implant surface are two important characteristics for osseointegration [2–4]. A moderately rough surface ($1 < Ra < 2\,\mu m$) has been shown to improve the formation of new bone and to increase the removal torque of the implant compared to a smoother one ($Ra < 1\,\mu m$) [3]. This phenomenon can be explained by the better implant anchorage in the jawbone related to a higher contact surface area between the implant and the bone tissue due to surface roughness [3,2]. It has also been shown that a highly rough surface ($Ra > 2\,\mu m$) leads to a poorer osseointegration and would induce a higher risk of bacterial colonization [4]. Interestingly, a highly hydrophilic surface (contact angle of 0°) seems to increase alkaline phosphatase activity and osteocalcin and generates an osteogenic microenvironment through higher production of prostaglandin E2 (PGE2) and transforming growth factor beta 1 (TGF-β1) [5]. In order to improve implant surface characteristics, surface treatments have been developed. For example, sandblasting, acid etching or anodization can be used [6]. Sandblasting treatments using Al_2O_3 or TiO_2 particles create a rougher surface ($0.5 < Ra < 2.0\,\mu m$) than acid etching ($0.3 < Ra < 1\,\mu m$). These two processes are commonly used jointly by implant manufacturers [7] and are collectively known as sandblasting large grit and acid etching (SLA). All of these surface treatments have shown osseointegration improvement [8,9]. Surface wettability depends on these surface treatments. For example for grade 4 unalloyed Ti implant, the contact angle measured using water was equal to $85° \pm 4°$ for a machined surface, $96° \pm 9°$ for an etched one, $80° \pm 5°$ for a sandblasted one and $47° \pm 3°$ for an anodized surface [8]. Moreover, wettability depends also on surface chemistry. A chemically modified SLA (modSLA) has been developed, with sandblasting and acid etching performed and then samples rinsed under nitrogen protection to prevent exposure to air and then stored in a sealed glass tube containing an isotonic NaCl solution. These steps lead to a strongly hydrophilic surface. It has been shown that bone healing was improved in the early stages after implantation, resulting in a removal torque 8–21% higher for a modSLA surface than for the conventional SLA one [10]. This has been explained by the pro-osteogenic and pro-angiogenic influence of this surface on gene expression a few days after implantation [11].

Another solution that has been largely developed to improve osseointegration of titanium implants is the use of calcium phosphate coated implants. To produce this coating, several processes have already been proposed, including plasma spraying, electrophoretic deposition, pulsed laser deposition and the soaking process [12,13]. Among these, plasma spraying, which is a high temperature process, is one of the most industrially used techniques to deposit hydroxyapatite on orthopedic implants because of its high efficiency and moderate cost. However, the resulting coating is thick ($>50\,\mu m$) and made of mixtures of phases with different dissolution rates due to the thermal decomposition of hydroxyapatite (HAP) that could lead to coating delamination [14]. In contrast, soaking process is a low temperature wet process that leads to thin coatings ($<10\,\mu m$) that can easily cover complex shapes and allow coating functionalization with thermosensitive molecules (growth factors, antibiotics and so on) [15]. Moreover, this soft deposition method is very versatile and allows for various calcium phosphates formation, i.e. octacalcium phosphate [16] or biomimetic carbonated apatite coatings [17] depending on experimental conditions. Some of these CaP phases, once implanted can dissolve leading to a local increase of biological fluid supersaturation with respect to calcium and phosphates that could help bone neoformation [18]. The soaking process most generally used to produce CaP coatings on metallic [19,20] or polymeric implants [21,22], or to form inorganic/organic composites [23,24], often involves simulated body fluid (SBF), a metastable supersaturated solution with the ability to precipitate only a minute amount of CaP salt (~150 mg of apatite per liter of solution at best). In addition, this process can take several hours or days to obtain a coating, depending on the crystal nucleation ability of the surface to coat [25]. To increase the deposition kinetics and the amount of CaP formed, some studies have been completed with higher ion concentrations (SBF ×2, ×5 or ×10) [17,19,26]. However at high supersaturation, CaP precipitates spontaneously in the solution, and thus, the efficiency of the coating formation is lower and its characteristics are difficult to control. Furthermore, the preparation and industrial use of large quantities of metastable solutions is problematic due to uncontrolled spontaneous precipitation in solution or on any surface of the equipment or materials. To prevent those drawbacks, an alternate soaking process, using two separated calcium and phosphate baths, has been developed. Briefly, several protocols have been reported in the literature, with the implant immersed in a calcium bath and, then rinsed and immersed in the phosphate bath and finally rinsed a second time. The immersion time varies from 1 min [23] to 1 h [24]. Moreover the coating thickness seems controllable by increasing the number of immersion cycles. Chemical surface treatment of the titanium substrate such as for example an alkaline surface treatment using NaOH has been proposed by some authors for improving the soaking and/or alternate soaking processes and particularly the CaP nucleation step [24,27,28].

It appears from this review of literature that all the titanium surface preparations coupled with an alternate soaking process already published used a NaOH pre-treatment to try to keep most of the calcium associated to the substrate during immersion in the baths and also during the rinsing step between the baths. In the present study, we chose to avoid

both steps (the NaOH chemical pre-treatment and the rinsing stage) and we propose another strategy by implementing only one additional step in the alternate soaking process to create a thin film of phosphate solution by centrifugation that can afterwards react with the calcium contained in the second bath to form a CaP coating.

The purpose of this study was to develop a surface treatment for titanium implants to obtain surface characteristics compatible with the formation of a homogeneous CaP bioactive coating using a low temperature alternate soaking process. The characterization of the effect of different protocols of acid etching on sandblasted titanium surfaces in terms of surface roughness, wettability, alumina particles embedding and mechanical properties was performed. Then the effect of identified crucial parameters for the centrifugation step on the CaP coating was studied using complementary physical and physico-chemical techniques. Finally, the adherence between the substrate and the coating was evaluated by a screwing/unscrewing test in an artificial jawbone.

2. Materials and methods

2.1. Sample preparation

All experiments were performed on samples with flat surfaces (cylindrical pieces of 15 mm long and 6 mm of diameter, each including 4 flat surfaces of 3 mm to facilitate their characterization before and after each treatment/step), and also on real dental implants. The substrate samples were all made of commercially pure grade 4 titanium (cpTi). Four different substrate surfaces were processed. The raw substrate surface corresponded to the machined surface and the associated sample was named M. Then, the machined samples were successively sandblasted with alumina particles (F100), leading to samples called S, which were then acid etched (SE samples). Two acid etching treatments were investigated. One etching treatment was performed in a special blend of acids composed of H_2SO_4:HCl:H_2O in 2:2:1 (vol %) proportion at 80 °C for 5 min and the resulting sample was called SE1. The second one, SE2, was based on a treatment in a mixed acid solution including H_2SO_4:HCl:H_2O in 3:1:1 (vol %) proportion at 40 °C for 20 min.

After the machining and sandblasting steps, the samples were degreased and cleaned with demineralized water and ethanol. After acid etching, the samples were first neutralized using a sodium bicarbonate solution and then rinsed with demineralized water and ethanol before being dried at 60 °C.

2.2. Soaking process

CaP coatings were deposited by a three-step soaking process. First, the titanium substrates were soaked in a phosphate solution (Na_3PO_4,12H_2O) at 0.5 M, during 30 min and at 37 °C. Then, a centrifugation step was realized using a Sigma 3–15 (Bioblock Scientific) and the effect of two parameters, the rotation speed (0–2000 rpm) and the centrifugation time (0–30 min), was investigated. The rotation speed was not tested below 500 rpm because of the device instability at low rotation speeds. Next, the samples were immersed in a calcium solution ($CaCl_2$,2H_2O) of 0.5 M, for 2 h at 80 °C. They were finally rinsed in two different baths of demineralized water and dried at room temperature.

2.3. Characterization

After each step of the surface preparation (machining, sandblasting and acid etching) and coating process, the sample surface was observed by SEM (LEO 435VP, ZEISS). SEM was performed both in secondary (SE) and backscattering (BSE) electron modes.

The SEM images in SE mode were recorded at a voltage of 15 KeV and a probe intensity of 150 pA to observe the surface morphology after surface treatment, as well as the microstructure and the coverage of the CaP coating. Two samples of each triplicate assay were observed to check the reproducibility of the coating process. Samples were embedded in an epoxy resin and then cross-sections were polished using silicon carbide (SiC) foils of reduced grit size from P180 (76 μm) to P2400 (10 μm). Five images were recorded to determine an average thickness value of the coating by image analysis.

BSE mode of SEM was utilized with a voltage of 15 KeV and a probe intensity of 1500 pA.

On the one hand, image analysis of SEM micrographs obtained in BSE mode was performed to determine the percentage of the titanium surface area corresponding to alumina particles embedded in the substrate after sandblasting and acid etching treatments. Four samples were studied after each acid etching treatment and ten images, with a size of 1024 × 888 pixels and a resolution of 205 dpi, were recorded for one sample. Image analysis was performed with *Image J* software. Manual thresholding of the BSE images was performed to obtain a binary image that gives indication of the ratio of the area covered by alumina particles to the total area of the image.

On the other hand, implant coverage by the coating was checked using the contrast between Ca, P and Ti elements in BSE mode.

The residual precursor salts that could remain on the coating were investigated by energy dispersive X-ray spectroscopy (EDX). The same voltage and intensity probe as in BSE mode were set and the acquisition time was equal to 100 s.

After each surface treatment, the roughness parameters, including arithmetical mean height (Sa), root mean square height (Sq), maximum height (Sz), skewness (Ssk) and kurtosis (Sku) of the 3D profile, were measured using a confocal and interferometric microscope (S Neox, SENSOFAR). These parameters are illustrated on 2D profiles in Fig. 1. For the acquisition, the interferometric mode, the ×10 microscope lens allowed for analysis of a surface of 1754 × 1320 μm, the green led and a scanning range along z axis of 40 μm were chosen. Moreover, before scanning, an auto-light and an auto-focus were performed on the sample surface. Three samples of the same batch for each surface treatment were analyzed and the reproducibility was checked by duplicating the characterization on another batch.

The wettability was also evaluated after each surface treatment by a contact angle measurement device (Digidrop, GBX). Each sample was cleaned with the same procedure before contact angle measurements to prevent any variability due to the history of the sample (variable times and/or conditions

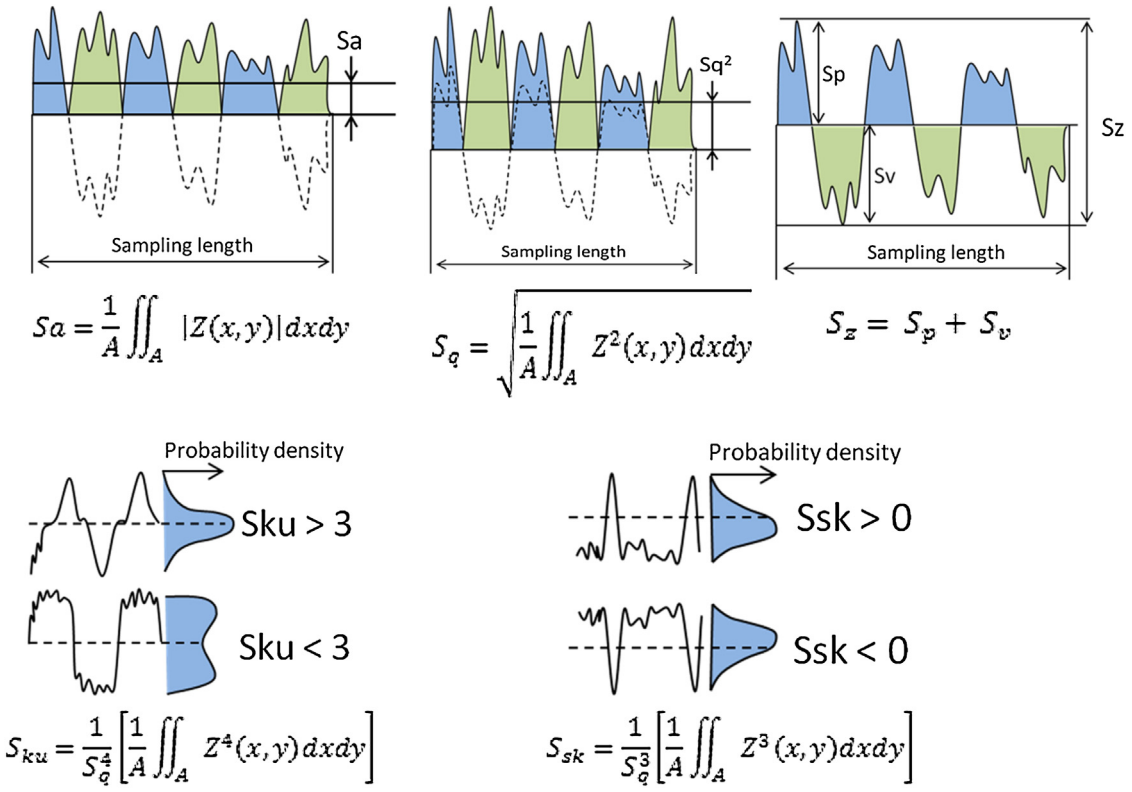

Fig. 1 – Illustration and formula related to the roughness parameters (adapted from Refs. [29] and [30]).

of storage before the measurements). This cleaning protocol applied to each sample includes: two rinsing baths in deionized water and one in ethanol (5 min of immersion in each bath in presence of ultrasounds) and then a drying step during 20 min at 60 °C. Ultrapure water (drop of 3 μL) was used for these experiments and a minimum number of twenty angles were measured per type of surface treatment. Dixon's test (5%) was applied to remove the outlier values.

Vickers hardness measurements (Omnimet 2100, BUEHLER) were performed after each step of the surface treatment. Samples were embedded in an epoxy resin and then cross-sections were polished using silicon carbide (SiC), as explained above, and finally using a colloidal silica suspension (OP-S, 0.04 μm) diluted with water in a proportion of 1/3 OP-S and 2/3 water. Indentation was performed with a load of 100 g and the diamond indenter remaining for 10 s in contact with the sample. A measurement was considered valid if the length of the measured diagonals was higher than 20 μm and if the difference of length between the two diagonals was less than 5% according to ISO 6507-2. Moreover, indentations were positioned at, at least, three times the diagonal length of the imprint from each other and from the sample edge. Indentations were performed close to the sample center and close to the edges. Three measurements were completed to determine the average hardness and the associated standard deviation.

Concerning the physico-chemical characterization of the coating, the first step was to check the presence of calcium and phosphate in the coating. Then, the goal was to determine what type(s) of calcium phosphate phase(s) was formed on the surface. With the experimental conditions (pH and T) and according to the literature [31], brushite (DCPD), octacalcium phosphate (OCP) or non-stoichiometric apatite analogous to bone mineral (ns-HAP) are the CaP phases that could potentially precipitate. For this purpose, XRD and FTIR and Raman spectroscopy were used.

The calcium phosphate phase(s) in the coatings were investigated using an X-ray diffractometer (D8-Advance, BRUKER). This was used in grazing incidence mode (2°) to permit the analysis of the coating directly on the substrate. The X-ray diffractogram data were collected using a Cu anticathode (wavelength = 1.54184 Å), from $2\Theta = 3°$ to 75° with a step of 0.03° and a counting time of 6 s.

FTIR spectroscopy (FTIR spectrometer iS50, Nicolet) was performed in the middle infrared range. FTIR analysis was performed in the attenuated total reflectance mode (ATR) using a diamond crystal in order to analyze the CaP coatings directly on the substrate. Several points were analyzed to check the chemical homogeneity of the coating.

Raman spectroscopy combined with a confocal microscope (Labram HR 800, Yvon Jobin – HORIBA) allowed for a focus on a special area. A 532 nm laser source, an 1800 grooves/mm grating and a ×100 microscope objective were used for the acquisitions. Moreover, several areas were explored for homogeneity control.

X-ray diffractograms and FTIR and Raman spectra of the calcium phosphate reference compounds (brushite, octacalcium phosphate and non-stoichiometric hydroxyapatite (ns-HAP)) synthesized at the CIRIMAT Laboratory were recorded using the previously described analysis conditions.

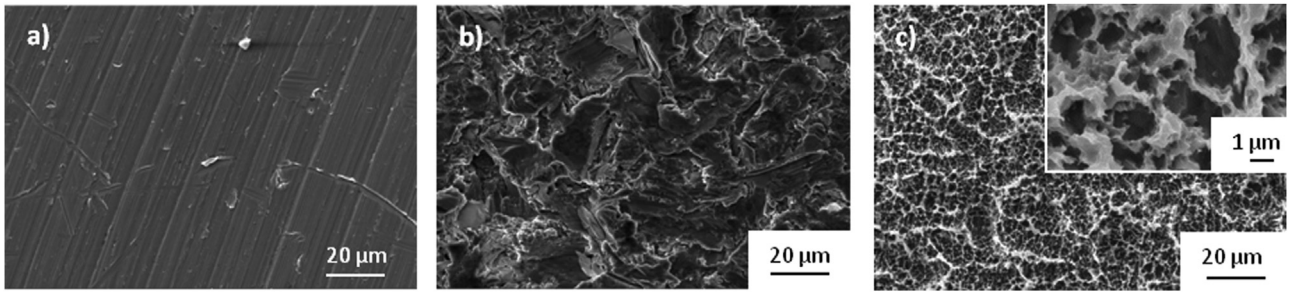

Fig. 2 – SEM micrographs of (a) machined surface (M), (b) sandblasted surface (S) and, (c) sandblasted and etched surface (SE2), inset at higher magnification.

The purity of synthesized OCP, ns-HAP and DCPD was verified by XRD by comparing the obtained diffractograms with JCPDS files n° 26-1056, n° 09-0432 and n° 09-0077, respectively.

Regarding the mechanical stability of the coating on the substrate, a screwing/unscrewing test was performed, consisting of mimicking an implantation procedure in an artificial jawbone. The model of mandible for implantology practice we used for the screwing/unscrewing test was provided by GF Dental (Milan, Italy). This model system is drilled and tapped according to the length and the diameter of the implant. Then, the coated implant was screwed, left 2 h in this artificial jawbone and then removed. The sample was then cleaned from artificial jawbone particles with compressed air. Finally, the implant surface was observed by SEM after this test.

3. Results

3.1. *Titanium substrate surface treatment*

The sample surface morphology was observed after each step of the process. The M substrate surface is flat and only the machining marks can be evidenced (Fig. 2a), leading to an anisotropically textured surface. After sandblasting, a surface roughness appeared (Fig. 2b) because alumina particles notched the titanium substrate surface and created substrate plastic deformation. Then, the acid solution etched titanium surface created micro-pits, on top of the previously formed roughness by sandblasting (Fig. 2c). Moreover, acid etching seems to lead to a more finely textured surface. The SE1 and SE2 treatments led to similar surface morphologies (data not presented).

Backscattered SEM observations revealed the presence of alumina particles (dark area) embedded in the titanium substrate after the sandblasting step (Fig. 3).

Image analysis on the BSE micrographs allows the estimation of the proportion of the Ti surface area covered by alumina particles after sandblasting, which is equal to $47 \pm 5\%$. It can be explained by the difference of hardness values between titanium and alumina, which are 215 HK [32] and 1800–2300 HK [33], respectively. This high proportion of alumina particles was found to be detrimental regarding the coating formation by our process. Nevertheless, the following steps of the surface preparation, which are acid etching and rinsing, enable an important reduction of alumina particles remaining embedded in the titanium substrate. Indeed the titanium surface covered by alumina particles decreases from $47 \pm 5\%$ after sandblasting to $6 \pm 4\%$ for SE1 and $3 \pm 2\%$ for SE2.

Afterwards, the roughness and wettability of each type of surface were measured and the results are reported in Table 1.

The major differences were observed between the machining and sandblasting steps. Indeed, the arithmetical mean height (Sa) and the root mean square height (Sq) are around five times higher for the sandblasted surface than for the machined one. The maximum height between the peak and valley (Sz) increases also by around four. The evolution of these latter parameters reflects a clear increase in the roughness after the sandblasting step. One important fact is the evolution of the surface skewness (Ssk) from positive to negative values between machined and sandblasted surfaces. Indeed Ssk expresses the symmetry of peaks and valleys relative to the average plane. If Ssk is positive, it is skewed downward, and if Ssk is negative, it is skewed upward. This means that machined samples are mainly composed of thin scratches

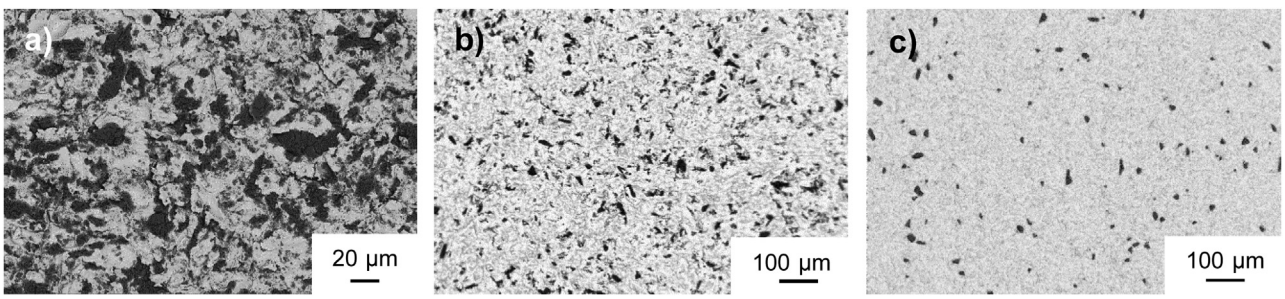

Fig. 3 – SEM micrographs obtained in backscattered electron mode of (a) sandblasted, (b) SE1 and (c) SE2 treated titanium surfaces.

Table 1 – Roughness parameters and contact angle measurements and their respective standard deviation after each type of surface treatment.

		Surface treatments			
		M	S	SE1	SE2
Surface characteristics	Sa (μm)	0.4 ± 0.1	1.8 ± 0.1	1.67 ± 0.09	1.46 ± 0.09
	Sq (μm)	0.4 ± 0.2	2.3 ± 0.1	2.1 ± 0.1	1.9 ± 0.1
	Sz (μm)	6 ± 1	23 ± 1	25 ± 6	21 ± 5
	Ssk	0.3 ± 0.1	−0.14 ± 0.05	−0.1 ± 0.1	−0.1 ± 0.1
	Sku	4 ± 2	3.4 ± 0.2	3.5 ± 0.6	3.4 ± 0.2
	Contact angle (°)	75 ± 7	50 ± 15	46 ± 19	0[a]

[a] Water droplet spreads totally on the surface leading to a low contact angle that is impossible to measure.

Table 2 – Vickers hardness measurements and their respective standard deviation after each type of surface treatment.

HV 0.1	M	SL	SE1	SE2
Close to the sample center	284 ± 9	273 ± 3	278 ± 1	275 ± 2
At 80 μm from the sample edge	278 ± 6	270 ± 7	280 ± 4	270 ± 7

due to the machining as already observed by SEM, whereas sandblasted samples exhibit wide craters due to the cutting effect of the sandblasting particles. The kurtosis (Sku) does not change for both surfaces and is higher than three, indicating the presence of sharp peaks. Then, acid etching leads to a decrease of Sa and Sq whereas Sz remains of the same order of magnitude. Acid etching seems to reduce the roughness by smoothing edges. Ssk is still negative and Sku higher than three. Comparing SE1 and SE2, a slight difference is observed for Sa and Sq values due to the difference in the etching protocols. No significant changes were observed for Sz, Ssk and Sku.

Concerning the contact angle, it can be observed that the machined surface has the highest contact angle (75 ± 7°) and thus the lowest wettability. The sandblasting step leads to a decrease of the contact angle (50 ± 15°). The SE1 surface is in the same order of magnitude than the sandblasted one. A very hydrophilic surface, for which the contact angle was impossible to measure because of the immediate droplet spreading (very low contact angle), was finally obtained after the SE2 surface treatment.

In order to highlight the influence of the different surface treatments on the substrate, the hardness was measured on two areas of the polished cross-sections of the samples, namely, the sample center and close to the edge (80 μm from the edge). Similar hardness values were recorded in these areas, whatever the surface state (machined, sandblasted and acid etched) (Table 2).

3.2. *Calcium phosphate coating using the soaking process*

Unlike the traditional soaking process where the substrate is the support for the nucleation of CaP crystals from a SBF or related supersaturated solutions [16,24,34], in the alternate soaking process presented in this study, the two first steps (phosphate bath immersion and centrifugation) are implemented to form a thin continuous phosphate solution film on the implant that can afterwards react with the calcium contained in the second bath to form a CaP coating. Thus, the critical step that plays a major role in the CaP coating formation is centrifugation, which determines the coating coverage and thickness. Therefore, several values of centrifugation time and rotations per minute were tested and are summarized in Table 3.

Table 3 – Occurrence of CaP coatings (reliability in %) on the titanium substrate depending on the centrifugation parameters (time and rotation speed): ● = coating fully covering the surface; # = coating not fully covering the surface; X = no coating.

RPM	Time					
	0 min	5 min	7 min	10 min	20 min	30 min
0	● 100%					
500		● 100%	● 80%	● 75%	#	
700		● 100%	● 80%		#	#
900		● 50%				#
1500		#	#		#	
2000		X			X	

After each experiment, the samples were observed using SEM and the coating presence and coverage were checked. In Table 3, the centrifugation parameter couples, which favor the formation of a covering coating, corresponding to Fig. 4a, are shown by full circles. In that case, a reliability test was performed that consists in counting the number of samples that are fully covered over a total number of produced samples ($n \geq 12$). It should be noted that without centrifugation (0 min/0 rpm), a coating is always obtained but with a lot of agglomerates (Fig. 4b) that make the coating thickness inhomogeneous. The centrifuge parameter couples represented by hash symbols correspond to the conditions where the coating exists but does not entirely cover the substrate. This case is illustrated in Fig. 4c where the areas covered with a CaP coating appear darker than Ti substrate using backscattering electron mode. Finally, the crosses correspond to the parameter couples for which no coating was observed at any assay.

For this study, the centrifugation parameters of 500 rpm and 5 min allowed for homogeneous coverage without agglomeration and with good reproducibility. This coating can be observed at higher magnification in Fig. 5a. The substrate roughness is still visible, which means that the coating is thin and covers the treated surface. The coating thickness was estimated at 2–3 μm from SEM observation of a substrate-coating cross-section (Fig. 5b). Moreover, EDX analysis showed the presence of titanium and aluminum due to the substrate

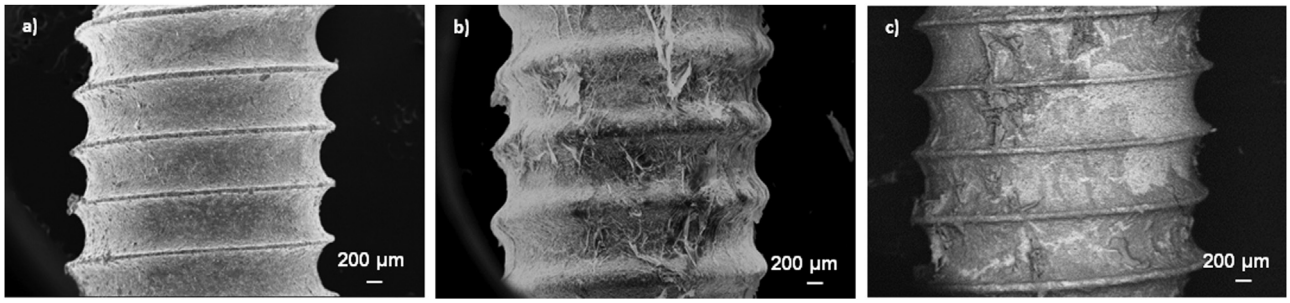

Fig. 4 – SEM micrographs of (a) a covering coating without agglomerates (SE mode), (b) a covering coating with agglomerates (SE mode) and (c) a non-covering coating (BSE mode).

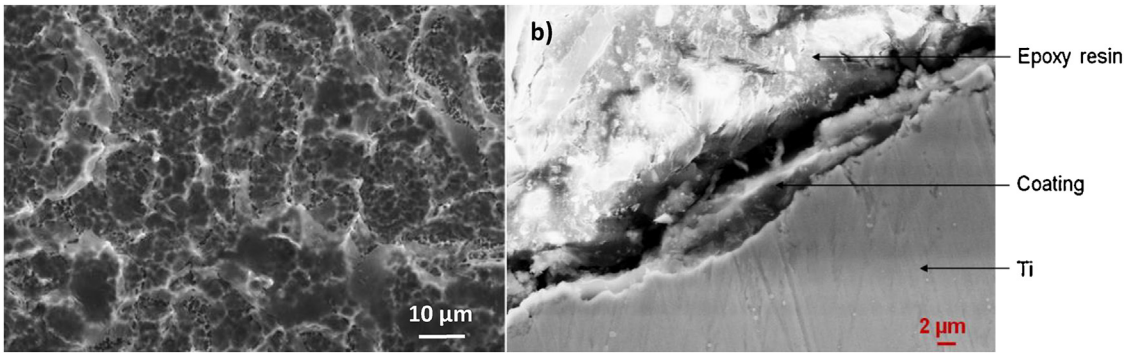

Fig. 5 – SEM micrographs of a SE2-treated sample after the soaking process: (a) surface and (b) polished cross-section.

and the alumina particles embedded, respectively (data not presented). It also showed the presence of calcium and phosphorus but no chlorine nor sodium which were the counter ions of calcium and phosphate salts used to prepare the soaking solutions. To establish the presence of a CaP coating, the crystalline phase and the chemical structure of the deposited material were also studied using XRD, FTIR and Raman spectroscopy.

The X-ray diffraction patterns of the three reference calcium phosphate compounds (ns-HAP, DCPD and OCP), as well as that of the coated sample, are shown in Fig. 6. Indeed, OCP has a characteristic peak at ≅4°, DCPD has one at ≅12° and apatite has few small peaks between 45° and 55° that do not correspond to OCP or DCPD. For the coated sample pattern, the main peaks at 35°, 38.5° and 40° are attributed to titanium and alumina, which are of the main components of the sandblasted substrate surface. This confirmed that the coating is thin and that some sandblasting particles are still embedded in the titanium substrate, even after acid etching, as previously shown in the SEM micrographs presented in Fig. 3b and c. The most intense peak of the OCP at ≅4° and of the DCPD at ≅12° are not observed for the coated sample, which could indicate the absence of these phases, even if the strong diffuse background, especially intense at low diffraction angles (background corrected in Fig. 6), would reduce their detection. However, a broad weak peak at ≅32° corresponding neither to titanium nor to alumina is identified that could be attributed to poorly crystalline OCP or ns-HAP diffraction peaks. The low intensity of this peak is probably due to the thinness of the coating and its poor crystallinity. Moreover, two peaks at ≅41° and 59.4° were identified that have been already observed in previous works and assigned to TiH_2 pro-

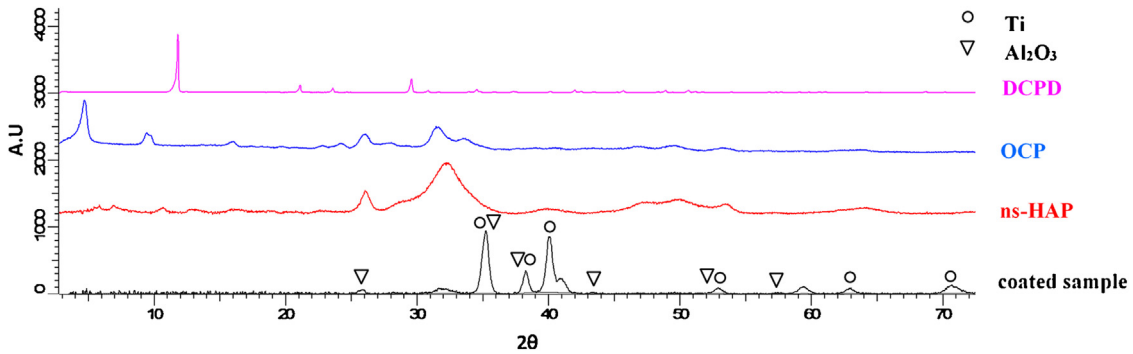

Fig. 6 – X-ray diffractograms of ns-HAP, DCPD, OCP reference compounds and of the coated sample.

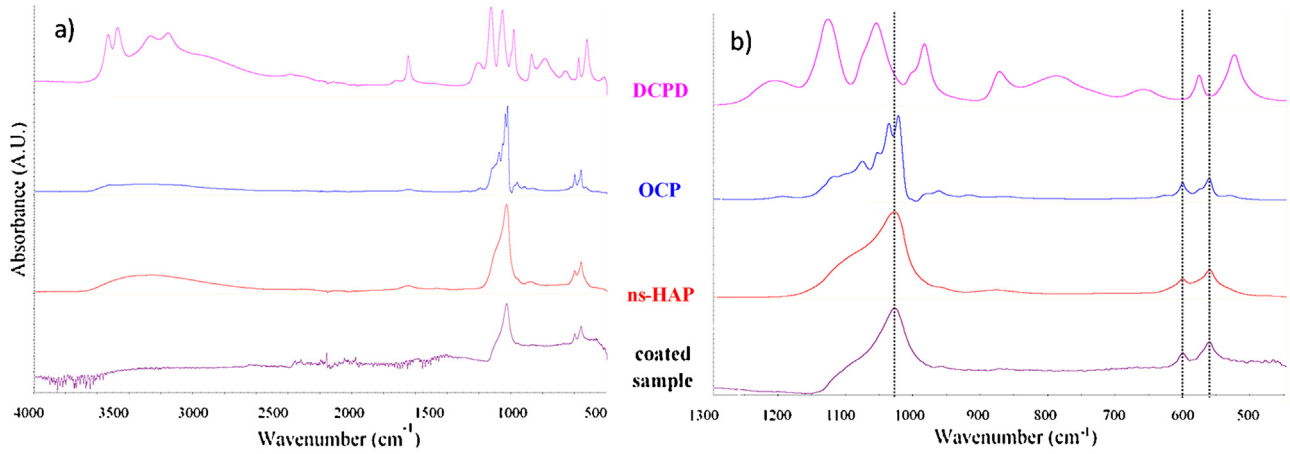

Fig. 7 – FTIR-ATR spectra of DCPD, OCP, ns-HAP reference compounds and coated sample: (a) full spectrum (4000–400 cm^{-1}) and (b) 1300–450 cm^{-1} domain.

duced during the etching reaction of titanium with sulfuric acid [28,35–37]. The same peaks were observed on XRD diffractogram of an uncoated etched sample. Also, these two peaks correspond to the most intense ones on the JCPDS file n° 09-0371 that support our hypothesis.

In the present study, the detection of CaP phases has to be confirmed using a complementary technique due to the weakness of the XRD peak(s) assigned to the CaP coating, blurred by the strong peaks due to the well crystallized substrate components (titanium and alumina).

The ATR-FTIR spectra of ns-HAP, DCPD, OCP and of the coated sample are shown in Fig. 7. The absence of the strongest bands corresponding to the ν_3 PO_4^{3-} vibration modes at 1132, 1070–1060 and 984 cm^{-1} and of a smaller one corresponding to the ν_4 PO_4^{3-} vibration mode at 525 cm^{-1} of the DCPD supports the hypothesis of the absence of this CaP phase in the coating.

The CaP-coated sample spectrum is similar to the one of the ns-HAP reference compound because of the shoulder between 1050 and 1150 cm^{-1} (ν_3 PO_4^{3-}), as well as the two bands at 560 and 601 cm^{-1} (ν_4 PO_4^{3-}), which could also be attributed to OCP. It is, once again, difficult to conclude the identification of the calcium phosphate phases. Even if the presence of ns-HAP seems possible, OCP could also take part in the coating composition. Indeed, it is difficult to distinguish these two calcium phosphate phases because the chemical structures of ns-HAP and OCP lead to close spectra and also, the resolution of the coated sample spectrum is low. The coating thickness, its poor crystallinity and substrate roughness are limiting attributes for a thorough characterization of the CaP-coated samples in ATR mode because of the difficulty to have a good contact between the diamond crystal of the ATR device and the sample surface.

Regarding the Raman spectroscopy analysis (Fig. 8), the strongest peak for the CaP-coated sample spectrum appeared at ≅962 cm^{-1}, which is a characteristic band of the ν_1 PO_4^{3-} vibration mode in OCP and ns-HAP (this band position is very close for both of these calcium phosphate phases). For DCPD, this peak would be observed at 986 cm^{-1}; its absence excludes the formation of DCPD which confirms the FTIR spectroscopy and XRD results.

The spectral resolution is not sufficient to distinguish the two peaks of OCP at 958 and 966 cm^{-1}. Due to the low reso-

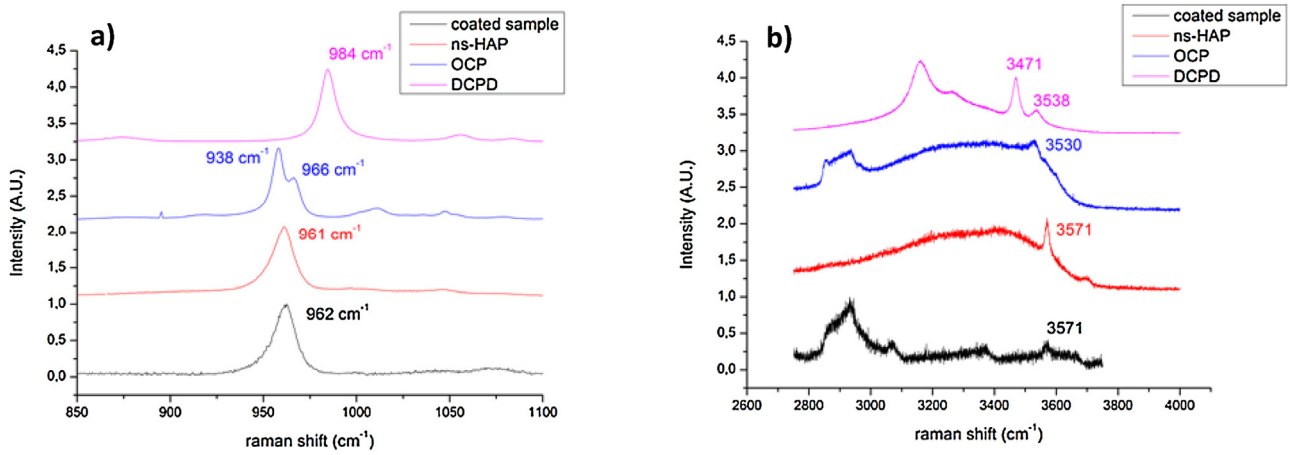

Fig. 8 – Raman spectra of ns-HAP, OCP, DCPD and CaP-coated sample: (a) 850–1100 cm^{-1} and (b) 2600–4000 cm^{-1} domains.

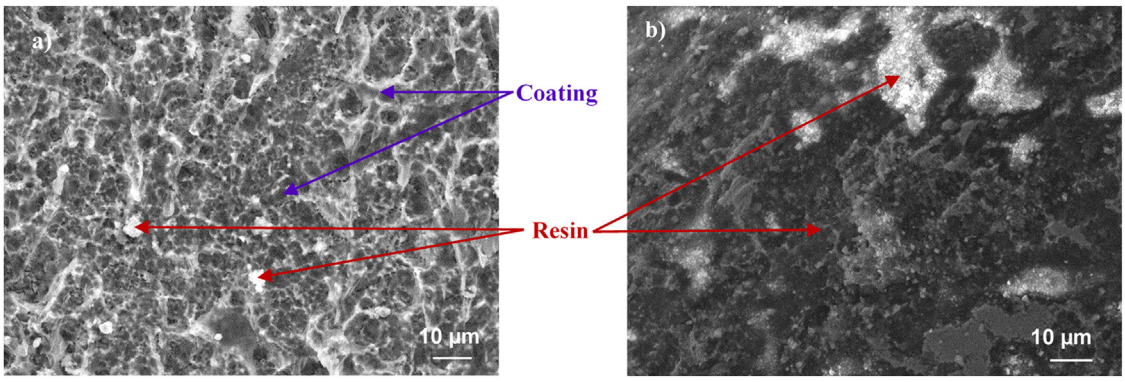

Fig. 9 – SEM micrographs of the Ca-P-coated implant surface after the screwing/unscrewing test (a) at the thread bottom and (b) at the thread top.

lution and the low intensity of the smallest peaks of OCP at 966 cm^{-1}, a clear identification and discrimination between ns-HAP and OCP compounds is difficult for these phases with closely related structures. Nevertheless, the medium peak of OCP standard at 1011 cm^{-1}, corresponding to the ν_3 PO_4^{3-} vibration mode did not appear on the CaP-coated sample spectrum (Fig. 8a). Moreover, the peak at 3575 cm^{-1} corresponding to the OH^- of the ns-HAP was observed on the CaP-coated sample spectrum, which can testify for the presence of ns-HAP in the coating (Fig. 8b). Therefore, Raman spectroscopy indicates that ns-HAP is a constituent of the CaP coating on the titanium substrate.

We also performed roughness and wettability measurements on CaP coated samples. The results showed that the roughness was not significantly modified after the coating and we were not able to measure a contact angle due to immediate droplet spreading (very low contact angle) as after SE2 treatment, indicating a highly hydrophilic surface of CaP-coated samples.

After the mechanical test of screwing and unscrewing the coated implant in an artificial jawbone, no damage was noticed at the thread bottom of the implant (Fig. 9a) but some particles which do not contain calcium, phosphorus or titanium according to EDX analysis (data not presented), can be observed above the coating. These particles are some debris of the artificial jawbone that remained stuck to the implant. The thread top was entirely covered by the resin of the artificial jawbone (Fig. 9b) which makes impossible the observation of the coating. Nevertheless we can suppose that the coating is still below this resin layer.

4. Discussion

Two protocols of surface preparation, including sandblasting with alumina particles and acid etching, were developed. During these surface treatments, the most critical step was the acid etching because it allowed a surface topography modification and an almost complete elimination of alumina particles embedded in the titanium substrate. Therefore, the parameters associated with this step, temperature and immersion time, which control the kinetics of the etching reaction, are important. The higher the temperature; the lower the immersion time to obtain the same surface topography after etching. Therefore, a compromise between temperature and immersion time has to be found to obtain an etched surface, while keeping the main roughness created by sandblasting. It has been shown that both investigated treatments, SE1 and SE2, allow a decrease in the amount of alumina particles on the titanium surface from ≅50% after sandblasting to ≅5% after acid etching. Moreover, hardness measurements have shown no significant changes after each surface treatment, which means no mechanical change of the titanium substrate. Therefore, acid etching leads to a clean and rough surface able to receive a bioactive calcium phosphate coating.

The acid etching processes tested include two temperatures, 40 °C and 80 °C, associated with two immersion times, 20 and 5 min, respectively. We showed that these two protocols associated with the sandblasting led to a rough surface with an average roughness between 1 and 2 µm and micro-pits that are considered as more favorable for osseointegration, compared to machined surfaces [38]. In addition to this, the SE2 surface showed a very high wettability (contact angle below the measurable limit compared to 46° and 50° for the SE1 and S samples, respectively) that is also an interesting advantage for osseointegration if the implants are used without coating [5] and probably also for the wet coating process carried on in this work. Moreover, XPS analyses demonstrated that chemical composition of SE1 and SE2 surfaces were similar (data not presented). Therefore, the difference observed in the hydrophilicity of these two surfaces is most probably due to variation in their surface topographical characteristics.

The main drawbacks of an etching process at high temperature, like SE1, are energy consumption, the change of bath composition due to evaporation and higher risk and security management within the framework of an industrial development. The SE2 surface treatment seems more adapted for the soaking process than sandblasting alone and SE1 surface preparations for several reasons. On the one hand, a high wettability is necessary to favor the development of a thin homogeneous phosphate solution layer in contact with the implant surface and to prevent the formation of inhomogeneous coating. On the other hand, the roughness and micro-pits achieved could trap more efficiently the phosphate solution and thus promote in-pores precipitation during the

coating formation, with a possible improvement of the coating mechanical adhesion. Regarding the characteristics of the surface obtained with the two acid etching protocols, the ability to form a CaP coating through the soaking process and industrial transfer considerations, it appears that the acid etching protocol at 40 °C for 20 min (SE2 protocol) is the best suited for the titanium surface preparation.

The main objective of the present study was to develop a soaking process that can avoid the problems due to the use of a supersaturated CaP solution as in the concentrated SBF soaking process. Moreover, to speed up the process without the use of complex and numerous chemical surface treatments a centrifugation step was introduced which generates a thin phosphate solution layer at the surface of the titanium substrate that when immersed in the following calcium bath allows for the precipitation of a thin and covering CaP coating. This step is crucial because it seems to determine the formation of the coating, its thickness and homogeneity. For this purpose, the phosphate solution has to be spread homogeneously on the substrate, which has to exhibit a high wetting ability as discussed earlier, to prevent inhomogeneous coverage. The rotation speed and centrifugation time are therefore critical parameters to control. Centrifugation must not lead to the elimination of the liquid phosphate solution film or recrystallization of the phosphate source salt by drying, which would prevent the following aqueous precipitation reaction with calcium ions in the second bath. These phenomena can happen for high centrifugation times and rotation speeds that do not lead to coating formation. In contrast, without centrifugation, the presence of agglomerates has been assigned to the uncontrolled thickness of the initial phosphate film, leading to uncontrolled precipitation of CaP weakly bound to the surface. The centrifugation parameters best adapted to produce a thin and covering CaP coating on the SE2 surface without agglomeration are 500 rpm for 5 min in our experimental conditions. We showed that a thin coating (thickness of 2–3 μm) was formed on the titanium substrate. This thinness allows the coating to follow the surface roughness created by the previously described surface treatments without changing its characteristics. This can be an important point for osseointegration and mechanical anchoring of the implant in bone, as explained earlier. We finally demonstrated that the CaP coating deposited using these parameters is also 100% reproducible.

A clear identification of the coating phase composition was difficult due to its thinness and its poor crystallinity. The absence of DCPD was demonstrated by XRD, FTIR and Raman spectroscopy. The coating seems more likely composed of ns-HAP due to the absence of the characteristic peak of OCP at ≅5° in the X-ray diffraction diagram and of the characteristic phosphate band at ≅966 cm^{-1} on the Raman spectrum. Moreover it is in accordance with the literature where, using an alternate soaking process on titanium and titanium alloys substrates, apatite [28] or octacalcium phosphate [16] were obtained. In any case as ns-HAP and/or OCP are metastable phases in physiological conditions, by similarity with previous work it can be concluded that the coating obtained would probably improve the implant osseointegration [20,39,40].

The mechanical stability of the coating has been demonstrated and is probably due to mechanical anchorage of the coating to the substrate thanks to the implant surface roughness generated by the sandblasting and the acid etching and thin layer precipitation in the well-spread phosphate solution film layer. Artificial jawbone debris stuck at the implant thread top could come from the warming at the implant/jawbone interface during screwing and unscrewing that can partly melt the plastic.

5. Conclusion

Thanks to complementary physical and physico-chemical techniques, this study showed that titanium implant surface characteristics can be optimized in terms of roughness and wettability by a surface preparation involving a sandblasting and an acid etching to improve its ability to receive a CaP coating formed at low temperature through an alternate soaking process and for the first time without any NaOH chemical pretreatment of the implant surface. SE2 preparation led to an average roughness between 1 and 2 μm and a high wettability (contact angle below the detection limit). Then, we determined the optimal centrifugation parameters (rotation speed and time) allowing to obtain a thin, homogeneous and adherent non-stoichiometric hydroxyapatite coating using an alternate soaking process applied to titanium dental implants. This process is rapid, reproducible and the resulting CaP coating is expected to favor early implant osseointegration through coating dissolution in vivo. In addition, this process should allow the easy association of biological active molecules and/or elements with the coating to also confer other functionality to the coating, for example, the prevention of post-operative infections.

Acknowledgments

The authors thank the Midi-Pyrénées Region (BIOACTISURF project n°14054394) for supporting this research work. They also thank Guillaume GODEFROY for his contribution in this work as an intern from the Université de Technologie de Compiègne at the CIRIMAT laboratory.

REFERENCES

[1] Albrektsson T, Brånemark P-I, Hansson H-A, Lindström J. Osseointegrated titanium implants: requirements for ensuring a long-lasting, direct bone-to-implant anchorage in man. Acta Orthop 1981;52(2):155–70.
[2] Rupp F, Liang L, Geis-Gerstorfer J, Scheideler L, Hüttig F. Surface characteristics of dental implants: a review. Dent Mater 2018;34(1):40–57.
[3] Wennerberg A, Ektessabi A, Albrektsson T, Johansson C, Andersson B. A 1-year follow-up of implants of differing surface roughness placed in rabbit bone. Int J Oral Maxillofac Implants 1997;12(4):486–94.
[4] Wennerberg A, Albrektsson T. Effects of titanium surface topography on bone integration: a systematic review. Clin Oral Implants Res 2009;20:172–84.
[5] Zhao G, Schwartz Z, Wieland M, Rupp F, Geis-Gerstorfer J, Cochran DL, et al. High surface energy enhances cell response to titanium substrate microstructure. J Biomed Mater Res A 2005;74A(1):49–58.

[6] Bagno A, Bello CD. Surface treatments and roughness properties of Ti-based biomaterials. J Mater Sci Mater Med 2004;15(9):935–49.
[7] Ballo AM, Palmquist A, Omar O, Xia W. Dental implant surfaces-physicochemical properties, biological performance, and trends, implant dentistry — a rapidly evolving practice. InTech 2011:19–56.
[8] Elias CN, Oshida Y, Lima JHC, Muller CA. Relationship between surface properties (roughness, wettability and morphology) of titanium and dental implant removal torque. J Mech Behav Biomed Mater 2008;1(3): 234–42.
[9] Wong M, Eulenberger J, Schenk R, Hunziker E. Effect of surface topology on the osseointegration of implant materials in trabecular bone. J Biomed Mater Res 1995;29(12):1567–75.
[10] Ferguson SJ, Broggini N, Wieland M, de Wild M, Rupp F, Geis-Gerstorfer J, et al. Biomechanical evaluation of the interfacial strength of a chemically modified sandblasted and acid-etched titanium surface. J Biomed Mater Res A 2006;78A(2):291–7.
[11] Donos N, Hamlet S, Lang NP, Salvi GE, Huynh-Ba G, Bosshardt DD, et al. Gene expression profile of osseointegration of a hydrophilic compared with a hydrophobic microrough implant surface. Clin Oral Implants Res 2011;22(4):365–72.
[12] Ben-Nissan B, Choi AH, Roest R, Latella BA, Bendavid A. 2 — Adhesion of hydroxyapatite on titanium medical implants. In: Mucalo M, editor. Hydroxyapatite (Hap) for biomedical applications. Woodhead Publishing; 2015. p. 21–51.
[13] De Groot K, Wolke JGC, Jansen JA. Calcium phosphate coatings for medical implants. Proc Inst Mech Eng H 1998;2:137–47.
[14] Le Guéhennec L, Soueidan A, Layrolle P, Amouriq Y. Surface treatments of titanium dental implants for rapid osseointegration. Dent Mater 2007;23(7):844–54.
[15] Layrolle P. 1.16 Calcium phosphate coatings. In: Comprehensive biomaterials II. Elsevier; 2017. p. 360–7.
[16] Barrere F, Layrolle P, Van Blitterswijk CA, De Groot K. Biomimetic coatings on titanium: a crystal growth study of octacalcium phosphate. J Mater Sci Mater Med 2001;12(6):529–34.
[17] Habibovic P, Barrère F, Van Blitterswijk CA, de Groot K, Layrolle P. Biomimetic hydroxyapatite coating on metal implants. J Am Ceram Soc 2002;85(3):517–22.
[18] Surmenev RA, Surmeneva MA, Ivanova AA. Significance of calcium phosphate coatings for the enhancement of new bone osteogenesis — a review. Acta Biomater 2014;10(2):557–79.
[19] Barrere F, Layrolle P, Van Blitterswijk CA, De Groot K. Biomimetic calcium phosphate coatings on Ti6Al4 V: a crystal growth study of octacalcium phosphate and inhibition by Mg^{2+} and HCO_3^-. Bone 1999;25(2): 107S–11S.
[20] Habibovic P, Li J, ven der Valk CM, Meijer G, Layrolle P, van Blitterswijk CA, et al. Biological performance of uncoated and octacalcium phosphate-coated Ti6Al4 V. Biomaterials 2005;26(January (1)):23–36.
[21] Goldberg AJ, Liu Y, Advincula MC, Gronowicz G, Habibovic P, Kuhn LT. Fabrication and characterization of hydroxyapatite-coated polystyrene disks for use in osteoprogenitor cell culture. J Biomater Sci Polym Ed 2010;21(10):1371–87.
[22] Taguchi T, Muraoka Y, Matsuyama H, Kishida A, Akashi M. Apatite coating on hydrophilic polymer-grafted poly(ethylene) films using an alternate soaking process. Biomaterials 2000;22(1):53–8.
[23] Strange DGT, Oyen ML. Biomimetic bone-like composites fabricated through an automated alternate soaking process. Acta Biomater 2011;7(10):3586–94.
[24] Izawa H, Nishino S, Maeda H, Morita K, Ifuku S, Morimoto M, et al. Mineralization of hydroxyapatite upon a unique xanthan gum hydrogel by an alternate soaking process. Carbohydr Polym 2014;102:846–51.
[25] Koju N, Sikder P, Ren Y, Zhou H, Bhaduri SB. Biomimetic coating technology for orthopedic implants. Curr Opin Chem Eng 2017;15:49–55.
[26] Adawy A, Abdel-Fattah WI. An efficient biomimetic coating methodology for a prosthetic alloy. Mater Sci Eng C 2013;33(3):1813–8.
[27] Le VQ, Pourroy G, Cochis A, Rimondini L, Abdel-Fattah WI, Mohammed HI, et al. Alternative technique for calcium phosphate coating on titanium alloy implants. Biomatter 2014;4(January (1)):e28534.
[28] Kono H, Miyamoto M, Ban S. Bioactive apatite coating on titanium using an alternate soaking process. Dent Mater J 2007;26(2):186–93.
[29] Roughness (2D) parameter | Olympus IMS [WWW Document], n.d. URL http://www.olympus-ims.com/en/knowledge/metrology/roughness/2d_parameter/. [Accessed 8 June 2017].
[30] Paramètres de rugosité surfacique | Paramètres de rugosité de surface spécifiés par la norme ISO 25178 | KEYENCE International Belgium(Français) [WWW Document], n.d. URL http://www.keyence.eu/frfr/ss/products/microscope/roughness/surface/tab01_d.jsp. [Accessed 29 August 2017].
[31] Combes C, Rey C. Biomatériaux à base de phosphates de calcium. Tech Ing 2013;(avr).
[32] ASM. Material Data Sheet [WWW Document], n.d. URL http://asm.matweb.com/search/SpecificMaterial.asp?bassnum=mtu040. [Accessed 5 October 2017].
[33] FEPA ABRASIVES > Abrasives > Grains [WWW Document], n.d. URL https://www.fepa-abrasives.com/abrasive-products/grains. [Accessed 28 August 2017].
[34] Barrere F, Snel MME, van Blitterswijk CA, de Groot K, Layrolle P. Nano-scale study of the nucleation and growth of calcium phosphate coating on titanium implants. Biomaterials 2004;25(14):2901–10.
[35] Ban S, Iwaya Y, Kono H, Sato H. Surface modification of titanium by etching in concentrated sulfuric acid. Dent Mater 2006;22(12):1115–20.
[36] Hayakawa T, Kawashita M, Takaoaka GH. Coating of hydroxyapatite films on titanium substrates by electrodeposition under pulse current. J Ceram Soc Jpn 2008;116(1349):68–73.
[37] Iwaya Y, Machigashira M, Kanbara K, Miyamoto M, Noguchi K, Izumi Y, et al. Surface properties and biocompatibility of acid-etched titanium. Dent Mater J 2008;27(3):415–21.
[38] Albrektsson T, Wennerberg A. Oral implant surfaces: part 1 — review focusing on topographic and chemical properties of different surfaces and in vivo responses to them. Int J Prosthodont 2004;17(5):536–43.
[39] Barrère F. Biomimetic calcium phosphate coatings: physicochemistry and biological activity. Enschede: University of Twente; 2002. Host.
[40] Rigo ECS, Boschi AO, Yoshimoto M, Allegrini S, Konig B, Carbonari MJ. Evaluation in vitro and in vivo of biomimetic hydroxyapatite coated on titanium dental implants. Mater Sci Eng C 2004;24(5):647–51.